Surface patterning of soft polymer film-coated cylinders via an electric field



2009 J. Phys.: Condens. Matter 21 445006

(http://iopscience.iop.org/0953-8984/21/44/445006)

IOP Publishing Journal of Physics: Condensed Matter

J. Phys.: Condens. Matter **21** (2009) 445006 (8pp) doi:10.1088/0953-8984/21/44/445006

# Surface patterning of soft polymer film-coated cylinders via an electric field

**Bo Li, Yue Li, Guang-Kui Xu and Xi-Qiao Feng**[1]

AML, Department of Engineering Mechanics, Tsinghua University, Beijing 100084, People's Republic of China

E-mail: fengxq@tsinghua.edu.cn

Received 27 June 2009, in final form 24 September 2009
Published 15 October 2009
Online at stacks.iop.org/JPhysCM/21/445006

**Abstract**

Using the linear stability analysis method, we investigate the surface wrinkling of a thin polymer coating on a cylinder in an externally applied electric field. It is demonstrated that energy competition between surface energy, van der Waals interactive potential energy and electrostatic interaction energy may lead to ordered patterns on the film surface. The analytical solutions are derived for the critical conditions of both longitudinal and circumferential instabilities. The wavelengths of the generated surface patterns can be mediated by changing the magnitude of the electric field. Our analysis shows that the surface morphology is sensitive to the curvature radius of the fiber, especially in the micrometer and nanometer length scales. Furthermore, we suggest a potential approach for fabricating hierarchical patterns on curved surfaces.

(Some figures in this article are in colour only in the electronic version)

## 1. Introduction

Many natural biomaterials have hierarchical surface structures, which are of critical importance for their biological functions. For example, owing to their special surface microstructures, lotus and lady's mantle leaves have superhydrophobic and self-cleaning properties [1]. Water striders can effortlessly stand and jump on water since the hierarchical microstructures on their legs can remarkably enhance their water-repelling ability [2]. Inspired by these interesting phenomena, much effort has been directed towards biomimetic fabrication of surface microstructures of novel materials with superhydrophobic or other physical properties. In addition, surface patterning techniques have a wide range of applications in lithography, light-emitting displays, microelectronics and plastic electronics, smart adhesion, medical engineering and many other fields. As a promising technique, surface patterning can be achieved by destabilization of materials, mediated by intermolecular interactions (e.g. van der Waals force) or externally applied forces (e.g. a mechanical load). Surface instabilities and induced patterns, occurring spontaneously or in response to externally applied loads, also underlie various materials processing, function and reliability problems of technologically significant applications [3–10]. Besides mechanical forces, an electric field can also lead to the formation of surface/interface patterns on materials [11–13] and this phenomenon has attracted increasing interest [14–19].

Most previous studies have focused on morphological formation on a planar surface. Due to the effects of topological constraint and surface tension, however, the wrinkling patterns on curved surfaces exhibit some features distinct from those on planar surfaces. Recently, considerable attention has been given to the instability of curved surfaces, e.g. the surface instability of electrospun fibers [20] and other cylindrical and spherical surfaces [21–28]. However, three-dimensional pattern characteristics and instability mechanisms of curved surfaces under the simultaneous action of surface tension, electric field and van der Waals force remain elusive.

Pattern formation on a curved surface is of both theoretical and technological interest. On the one hand natural materials (e.g. water strider legs and plant seeds) usually have curved shapes; and on the other, devices and structures with various curved shapes (e.g. fibers and particles) are widely employed in advanced functional materials. Patterning a curved surface at the micro/nanoscale remains a challenging issue. In the present paper, we suggest an approach for fabricating micro/nanosized patterns on a cylindrical surface. The surface stability of a viscous thin film coated on a cylinder under

[1] Author to whom any correspondence should be addressed.

 

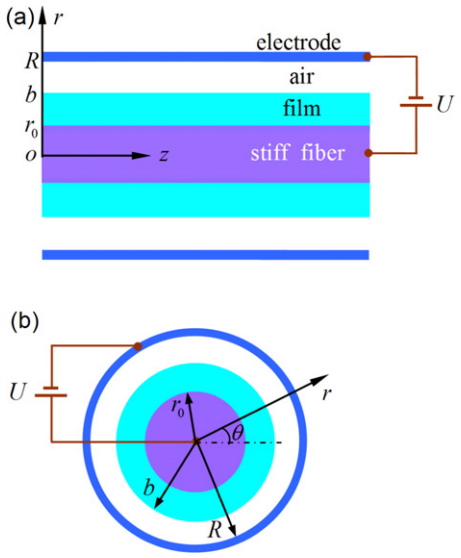


**Figure 1.** A viscous thin film lying on a stiff cylinder subjected to an externally applied electric field: (a) front view; (b) lateral view.

the action of an electric field is analyzed in section 2. Using linear electrohydrodynamic stability theory, the time-dependent evolution equation of the thin film surface and the critical conditions of surface wrinkling are analytically derived in section 3. The effects of electric field intensity, fiber curvature and surface tension on the induced surface patterns are examined in section 4. Finally, we discuss a biologically inspired technique to produce hierarchical surface patterns of materials.

## 2. Model and basic equations

### *2.1. Model*

Consider a very long and stiff cylinder coated with a conductive polymer film, surrounded by a tube-shaped electrode, as shown in figure 1. A voltage $U$ is applied between the cylinder and the electrode, creating an electric field perpendicular to the surface of the film. The dielectric constant of the air around the film is $\varepsilon_a$. During the patterning process, the polymer film is heated to a temperature above its glass transition temperature [15], and in this case it is usually treated as an extremely viscous fluid [12, 13]. Refer to a cylindrical polar coordinate system $(r, \theta, z)$, where the $z$ axis is aligned with the longitudinal direction. Let $r_0$ denote the radius of the fiber, $h_0$ the thin film thickness before wrinkling, and $R$ the inner radius of the electrode. Then, the outer radius of the film before wrinkling is $b = r_0 + h_0$, and the distance between the counter electrode and the undisturbed surface is $R - b$.

In general, the surface instability of thin films is of the long-wave type, that is, the characteristic length of the wave is much larger than the film thickness [11–13]. In this case, the surface evolution of the thin film can be written as [15, 16]

$$\frac{\partial h}{\partial t} = -\nabla \cdot \mathbf{j}, \tag{1}$$

where $\nabla$ denotes the gradient operator, $h$ is the film thickness after perturbation and $\mathbf{j}$ is the pressure-driven flux in the viscous polymer. Neglecting the viscosity of the air between the film and the electrode, $\mathbf{j}$ is related to the pressure $p$ by

$$\mathbf{j} = -\frac{1}{3\mu} h^3 \nabla p, \tag{2}$$

where $\mu$ is the viscosity of the polymer film. The pressure $p$ involves four contributions, including atmospheric pressure $p_0$, Laplace pressure $p_{\mathrm{Lap}}$, electrostatic pressure $p_{\mathrm{el}}$, and disjoining pressure $p_{\mathrm{dis}}$, i.e.

$$p = p_0 + p_{\mathrm{Lap}} + p_{\mathrm{el}} + p_{\mathrm{dis}}. \tag{3}$$

The Laplace pressure arises from the surface energy contribution due to the change of surface area, and is given by $p_{\mathrm{Lap}} = \gamma\kappa$, where $\gamma$ is the surface tension and $\kappa$ is the curvature of the film surface. The electrostatic pressure $p_{\mathrm{el}}$ originates from the Maxwell stress, which will be given in section 3. The disjoining pressure at the film surface stems from the van der Waals interaction between the film and the wettable fiber. It is expressed as $p_{\mathrm{dis}} = A/(6\pi h^3)$, with $A$ being the Hamaker constant [21].

### *2.2. Electric field*

The electric field intensity $\mathbf{E}(E_r, E_\theta, E_z)$ fulfills the Maxwell equations [29]

$$\nabla \cdot \mathbf{E} = \mathbf{0}, \qquad \nabla \times \mathbf{E} = \mathbf{0}, \tag{4}$$

in the air between the surface of the conductive film and the counter electrode. Construct a potential function $\phi$ such that

$$\mathbf{E} = -\nabla\phi. \tag{5}$$

Then the second equation in equation (4) is automatically satisfied and the first equation yields

$$\Delta\phi = 0, \tag{6}$$

where $\Delta$ is the Laplacian operator.

Under the action of the electric field, a Maxwell stress $\sigma_{\mathrm{M}}$ will arise at the surface of the thin film [29],

$$\sigma_{\mathrm{M}} = \tfrac{1}{2}\varepsilon_0\varepsilon_a\mathbf{E}_a^2, \tag{7}$$

where $\varepsilon_0$ is the dielectric permittivity of the vacuum. For a conductive film, the electric field affects the flow only through the Maxwell stress acting on the surface. In this case, the bulk of the viscous film is free of body charges.

## 3. Linear stability analysis

### *3.1. Physical fields in the undisturbed state*

In the undisturbed state, the electric potential $\bar{\phi}$, satisfying equation (6) and the symmetrical conditions, takes the following form $\bar{\phi} = \bar{c}\ln r + \bar{d}$, where $\bar{c}$ and $\bar{d}$ are two constants, which still need to be determined from the boundary conditions. Here and in the sequel, an overbar stands for a

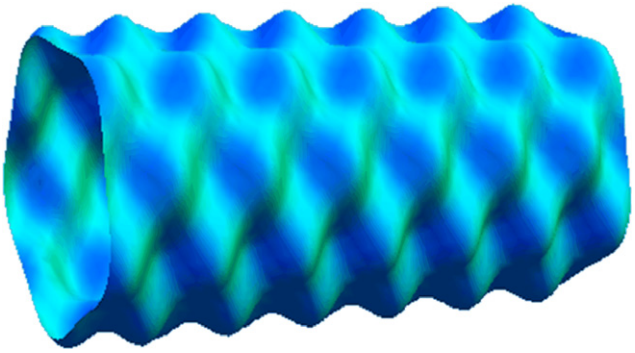

**Figure 2.** Three-dimensional morphology of surface instability on a cylindrical film.

quantity in the undisturbed state. These boundary conditions include $\bar{\phi}|_{r=b} = U$ and $\bar{\phi}|_{r=R} = 0$. Then the electric potential in the air is given by

$$\bar{\phi} = \frac{U}{\ln(R/b)} \ln \frac{R}{r}. \tag{8}$$

From equations (5) and (8), the nonzero component of the electric fields is then derived as

$$\bar{E}_r = \frac{U}{r \ln(R/b)}. \tag{9}$$

### 3.2. Linear stability analysis

In what follows, we will investigate the surface stability of the thin film by a linear instability analysis. For a very long cylindrical surface, there exist two possible types of surface instability, leading to longitudinal and circumferential patterns, respectively [28]. They may occur separately or simultaneously on a surface, depending upon the characteristic sizes (thin film thickness $h_0$ and fiber radius $r_0$), loading conditions, and mechanical properties of the thin film. The simultaneous occurrence of the two types of instability will lead to a three-dimensional surface pattern, as illustrated in figure 2. The critical condition of surface instability and the characteristic wavelength of the induced three-dimensional surface pattern will be derived.

Introduce the following sinusoidal perturbation over the surface of the thin film [28]:

$$\tilde{b}(\theta, z, t) = b + \delta(t) \cos(n\theta) \cos(\omega z), \tag{10}$$

where $\delta(t)$ is the amplitude of the perturbation, $n$ the mode-number in the circumferential direction, and $\omega$ the wavenumber in the axial direction. A tilde over a symbol stands for a quantity in the wrinkling state. For the linear stability analysis presented here, all non-linear terms of $\delta(t)$ can be neglected. Thus, the mean curvature on the film surface corresponding to the deformation in equation (10) is

$$\kappa = \frac{1}{b} + \left(\frac{n^2 - 1}{b^2} + \omega^2\right) \delta \cos(n\theta) \cos(\omega z). \tag{11}$$

The electric potential $\tilde{\phi}$ induced by the perturbation in equation (10) can be characterized in the form $\tilde{\phi} = \tilde{\phi}_r(r) \cos(n\theta) \cos(\omega z)$. Substituting this expression into equation (6) yields

$$\tilde{\phi} = [\tilde{c} I_n(\omega r) + \tilde{d} K_n(\omega r)] \cos(n\theta) \cos(\omega z), \tag{12}$$

where $\tilde{c}$ and $\tilde{d}$ are two constants still to be determined, and $I_n(\omega r)$ and $K_n(\omega r)$ are the first and second modified Bessel functions of the $n$th order, respectively. The total electric potential resulting from the perturbation and the externally applied voltage is written as $\phi = \bar{\phi} + \tilde{\phi}$ and the corresponding boundary conditions read $\phi|_{r=\tilde{b}} = U$ and $\phi|_{r=R} = 0$. Making use of equation (8) and eliminating the second-order terms of $\delta$, the constants $\tilde{c}$ and $\tilde{d}$ in equation (12) can be easily derived. Then the electric potential induced by the perturbation is given by

$$\tilde{\phi} = -\frac{U\delta}{b \ln(R/b)} \frac{K_n(\omega R) I_n(\omega r) - I_n(\omega R) K_n(\omega r)}{I_n(\omega R) K_n(\omega b) - I_n(\omega b) K_n(\omega R)} \times \cos(n\theta) \cos(\omega z). \tag{13}$$

From equations (5), (8) and (13), the electric field in the air can be obtained, but its lengthy expression is omitted here. Using equation (7), the Maxwell stress is calculated to the first order of $\delta$ as

$$\sigma_{\mathrm{M}} = \frac{\varepsilon_0 \varepsilon_{\mathrm{a}} U^2}{2b^2[\ln(R/b)]^2} \times \left\{1 + \frac{2\omega\delta[K_n(\omega R) I_n'(\omega b) - I_n(\omega R) K_n'(\omega b)]}{I_n(\omega R) K_n(\omega b) - I_n(\omega b) K_n(\omega R)} \times \cos(n\theta) \cos(\omega z)\right\}, \tag{14}$$

where the prime stands for the derivative with respect to the coordinate $r$. Then the electrostatic pressure $p_{\mathrm{el}}$ acting on the film surface equals $-\sigma_{\mathrm{M}}$, and the total pressure $p$ in equation (3) is determined as

$$p = \bar{p}_0 + \left[\gamma\left(\frac{n^2 - 1}{b^2} + \omega^2\right) - \sigma_{\mathrm{M0}} - \frac{A}{2\pi h_0^4}\right] \times \delta \cos(n\theta) \cos(\omega z), \tag{15}$$

where

$$\bar{p}_0 = p_0 + \frac{\gamma}{b} - \frac{\varepsilon_0 \varepsilon_{\mathrm{a}} U^2}{2b^2[\ln(R/b)]^2} + \frac{A}{6\pi h_0^3}, \tag{16}$$

$$\sigma_{\mathrm{M0}} = \frac{\varepsilon_0 \varepsilon_{\mathrm{a}} U^2 \omega}{b^2[\ln(R/b)]^2} \frac{K_n(\omega R) I_n'(\omega b) - I_n(\omega R) K_n'(\omega b)}{I_n(\omega R) K_n(\omega b) - I_n(\omega b) K_n(\omega R)}. \tag{17}$$

The pressure $\bar{p}_0$ represents the initial total pressure before wrinkling and, therefore, is independent of $n$ and $\omega$. It is seen from equation (16) that, at the initial state, the surface tension presses the film while the electrical stress and the van der Waals force ($A < 0$) induce negative pressures on the film surface. The second term in equation (15) is the total pressure excited by the perturbation. Substituting equation (15) into (1) and applying equations (2) and (11) leads to $\mathrm{d}\delta/\mathrm{d}t = \tau\delta$. Integrating this equation, the evolution equation of surface morphology after the initial perturbation is derived as $\delta(t) = \delta_0 \exp(\tau t)$, where $\delta_0$ denotes the perturbation amplitude at $t = 0$. $\tau$ is an important dimensionless parameter evaluating

the growth of surface evolution, also referred to as the growth rate. It is given by

$$\tau = \frac{\gamma h_0^3}{3\mu}\left(\frac{n^2}{b^2}+\omega^2\right)\left[\frac{1-n^2}{b^2}-\omega^2+\frac{\sigma_{M0}}{\gamma}+\frac{A}{2\pi\gamma h_0^4}\right]. \tag{18}$$

From equation (18), a critical state of the system can be defined by $\tau = 0$, and we denote the corresponding critical wavenumber as $\omega_c$ and the mode-number as $n_c$. If $\tau < 0$, the amplitude of the initial perturbation will decay exponentially with time, indicating that the film surface is stable with respect to the perturbation. When $\tau > 0$, on the other hand, the film is unstable and the perturbation amplitude will be exponentially magnified with time. In the latter case, due to the imbalance among the Laplacian, electrostatic and disjoining pressures acting on the film surface, the fluctuation with a particular longitudinal wavenumber and circumferential mode-number will be amplified, leading to the formation of an ordered surface pattern. The characteristic pattern corresponding to the fastest growth rate is regarded as the most probable mode to appear. In other words, one can predict its characteristic longitudinal wavenumber $\omega_m$ and circumferential mode-number $n_m$ from the following conditions:

$$\frac{\partial\tau}{\partial\omega}=0,\qquad \frac{\partial\tau}{\partial n}=0,\qquad \frac{\partial^2\tau}{\partial\omega^2}<0,$$
$$\frac{\partial^4\tau}{\partial\omega^2\partial n^2}-\left(\frac{\partial^2\tau}{\partial\omega\partial n}\right)^2>0. \tag{19}$$

Then the corresponding characteristic wavelengths in the longitudinal and circumferential directions are designated as $\lambda_{Lm} = 2\pi/\omega_m$ and $\lambda_{Cm} = 2\pi b/n_m$, respectively.

In the special case when only longitudinal surface wrinkling occurs, the growth rate $\tau_L$ can be readily obtained from equation (18) by setting $n = 0$. In the absence of the electric field, the characteristic longitudinal wavelength is explicitly derived as

$$\lambda_{Lm} = \frac{4\pi b h_0^2\sqrt{\pi\gamma}}{\sqrt{2\pi\gamma h_0^4 + Ab^2}}, \tag{20}$$

which describes the film surface pattern induced by spontaneous instability in the longitudinal direction. It is seen from equation (20) that the van der Waals force ($A < 0$) will partially counteract the effect of surface tension and consequently increase the wavelength. This spontaneous instability occurring on the surface of a thin fiber is different from that at a planar surface. For a thin film lying on a planar substrate the surface tension always plays a stabilizing role, while for the problem of current interest, the surface tension may drive the thin film to wrinkle due to the small curvature of the film surface. Therefore, the spontaneous instability of thin films is sensitive to the curvature of the underlying substrate. Furthermore, if the van der Waals interaction between the thin film and the fiber is further neglected, the wavelength in equation (20) corresponding to the fastest growth rate of $\tau_L$ reduces to $\lambda_{Lm} = 2\sqrt{2}\pi b$, which is identical to the wavelength of the classical Rayleigh instability [30]. This indicates that one can utilize spontaneous instability to fabricate ordered patterns on a thin polymer film surface. However, the use of an electric field will make the surface patterning process easier and, more importantly, allow us to mediate the characteristic dimensions of the surface morphology by varying such factors as the electric field intensity.

In another special case when only the circumferential surface wrinkling happens, the limit of equation (18) for $\omega \to 0$ gives

$$\tau_C = \frac{\gamma h_0^3 n^2}{3\mu b^2}\left[\frac{n\varepsilon_0\varepsilon_a U^2(R^{2n}+b^{2n})}{\gamma b^3[\ln(R/b)]^2(R^{2n}-b^{2n})}+\frac{A}{2\pi\gamma h_0^4}-\frac{n^2-1}{b^2}\right]. \tag{21}$$

Obviously, the first term in the square brackets, stemming from the externally applied electric field, always destabilizes the film surface. It is worth noticing that the individual circumferential instability ($\tau_C > 0$) occurs only when the voltage $U$ exceeds a certain critical value since the mode-number $n$ (integer) in equation (21) must be greater than 1 ($n = 1$ corresponding to the simple relative rotation of the film surface). In the absence of an electric field, the growth rate $\tau_C$ is always negative and, therefore, the spontaneous instability does not happen in the circumferential direction. Furthermore, for a large value of $n$ or $R \gg b$, the characteristic wavelength on the film surface can be explicitly derived as

$$\lambda_{Cm} = \left\{16\gamma b^2 h_0^2\pi^{3/2}[\ln(R/b)]^2\right\}\left\{3\sqrt{\pi}h_0^2\varepsilon_0\varepsilon_a U^2 + \sqrt{9\pi h_0^4\varepsilon_0^2\varepsilon_a^2 U^4 + 16\gamma b^2(2\pi\gamma h_0^4 + Ab^2)[\ln(R/b)]^4}\right\}^{-1}. \tag{22}$$

Equations (21) and (22) imply that increasing the voltage $U$ can amplify the growth rate of surface morphological evolution and reduce the characteristic wavelength $\lambda_{Cm}$.

## 4. Results and discussions

In section 3 we derived the surface evolution equation for a viscous film bonded on a stiff fiber in an electric field. In what follows, we will illustrate the prominent features of the longitudinal and circumferential instabilities in this system.

We normalize the growth rate $\tau$ as $\tau_0 = 3\mu b^4\tau/(\gamma h_0^3)$. Equation (18) shows that the dimensionless growth rate $\tau_0$ is a function of the wavenumber $\omega$ along the longitudinal direction and the mode-number $n$ along the circumferential direction, as shown in figure 3, where we take the representative values $\gamma = 0.015\ \mathrm{N\,m^{-1}}$, $h_0 = 100$ nm, $A = -20\times10^{-20}$ J, $d = 50$ nm [16, 31] and $r_0 = 1\ \mu$m. It is seen from figure 3(a) that the critical plane $\tau_0 = 0$ corresponds to a curve of critical modes $(n_c, \omega_c)$, at which the growth rate is zero. The surface of the thin film is unstable in the range of $\omega \in (0, \omega_c)$ and $n \in (0, n_c)$, i.e. above the critical plane $\tau_0 = 0$ in figure 3(a). The electric field serves as the main driving force of the instability. Due to the perturbation, the electrostatic pressure on the film surface will become nonuniform and its gradient drives the viscous fluid from the troughs to the crests

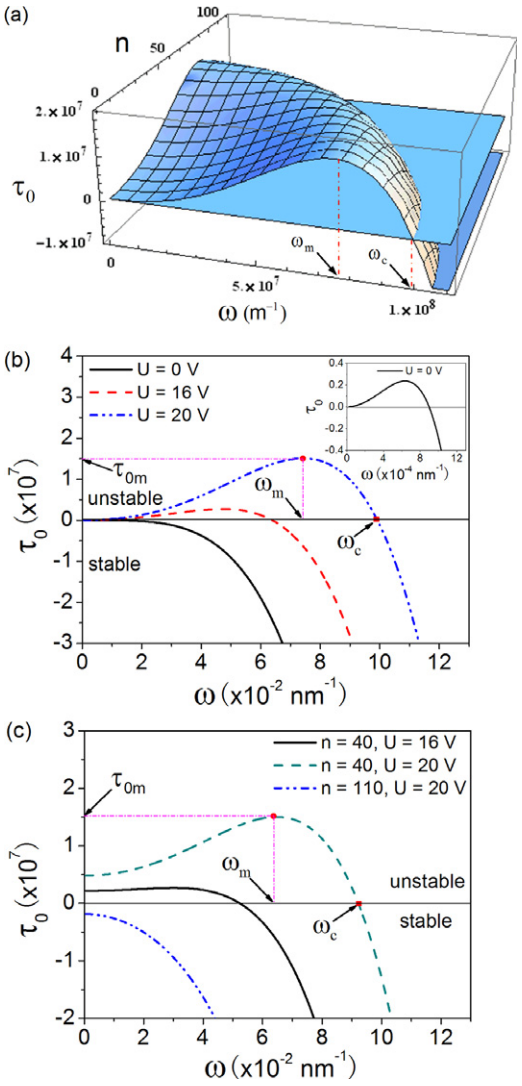


**Figure 3.** (a) Dependence of the growth rate $\tau_0$ on the wavenumber $\omega$ and mode-number $n$, where $U = 20$ V. (b) Dependence of the growth rate $\tau_0$ on the wavenumber $\omega$ for mode-number $n = 0$ and representative voltages $U$. (c) Dependence of the growth rate $\tau_0$ on the wavenumber $\omega$ for representative mode-number $n$ and voltages $U$.

and increases the amplitude of the perturbation. On the other hand, the van der Waals interaction between the film and the fiber will drive the matter from the crests to the troughs and play a surface stabilizing role. In addition, the surface tension, manifesting itself through the curvature term, may contribute to the Rayleigh-like instability of the thin film on a thin fiber.

Among all possible modes of bifurcation, the actual film surface will undergo the most probable one $(n_m, \omega_m)$, which holds the fastest growth rate of surface morphological evolution. Thus, competition between the electric force, surface tension and repulsive van der Waals force will yield a regular pattern on the surface of the curved film. Figures 3(b) and (c) show the variation of the growth rate $\tau_0$ with respect to the wavenumber $\omega$ for several circumferential mode-numbers $n$. It is seen that in the special case of $n = 0$, the growth rate $\tau_0$ approaches zero as $\omega \to 0$. The curve for $U = 0$ (also

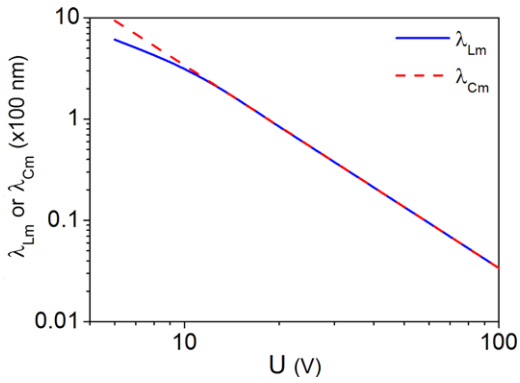


**Figure 4.** Dependence of the characteristic wavelengths $\lambda_{Lm}$ and $\lambda_{Cm}$ on the voltage $U$, where we take $h_0 = 50$ nm, $\gamma = 0.015$ N m$^{-1}$, $d = 50$ nm [18, 31] and $r_0 = 1$ $\mu$m.

refer to the inset at the top right of figure 3(b)), corresponds to spontaneous instability of the film surface. The critical wavenumber $\omega_c$ and the most probable wavenumber $\omega_m$ for this spontaneous instability are 0.90 $\mu$m$^{-1}$ and 0.64 $\mu$m$^{-1}$, respectively. As the externally applied voltage increases, the electric field gradually prevails over the surface tension and van der Waals interaction and dominates the surface patterning process. It is also seen from figure 3(b) that with increasing $U$, the growth rate for different voltages will exhibit a maximum and then become negative for $\omega$ larger than $\omega_c$. Both the critical wavenumber $\omega_c$ and the most probable wavenumber $\omega_m$ increase with the increase of $U$.

Figure 3(c) shows the results of circumferential instability. For a given mode-number $n$, a larger voltage will result in a faster growth rate and a larger most probable wavenumber. For $n = 40$, for example, $U = 16$ V and 20 V lead to $\omega_m = 30$ $\mu$m$^{-1}$ and $\tau_{0m} = 2.69 \times 10^6$, and $\omega_m = 64.7$ $\mu$m$^{-1}$ and $\tau_{0m} = 1.5 \times 10^7$, respectively. In addition, one can find that under a given voltage, the film surface is insensitive to the perturbation of sufficiently large $n$, as indicated by the curves of $n = 40$ and 110. Therefore, surface patterns with a relatively large wavenumber and mode-number are achievable by increasing the intensity of the electric field.

To further illustrate the influences of such factors as electric field and material properties on the surface pattern, we separately discuss the longitudinal (i.e. $n = 0$) and circumferential (i.e. $\omega = 0$) instabilities. For a given film thickness $h_0$, the variations of the characteristic wavelengths $\lambda_{Lm}$ and $\lambda_{Cm}$ with increasing $U$ are depicted in figure 4. Apparently, increasing the voltage significantly reduces both the characteristic wavelengths $\lambda_{Lm}$ and $\lambda_{Cm}$. Notwithstanding the surface tension spontaneously characterizes the film surface by Rayleigh-like instability and the van der Waals interaction enhances the corresponding wavelength, the surface pattern is mainly controlled by the external voltage. This salient feature inspires a feasible and controllable approach for patterning a curved surface. Moreover, when the applied voltage $U$ is large, $\lambda_{Lm}$ almost coincides with $\lambda_{Cm}$, while for a small $U$ they have a considerable difference. This is because when $U$ is relatively small, the instability happens mainly in the longitudinal direction and the surface tension dominates the

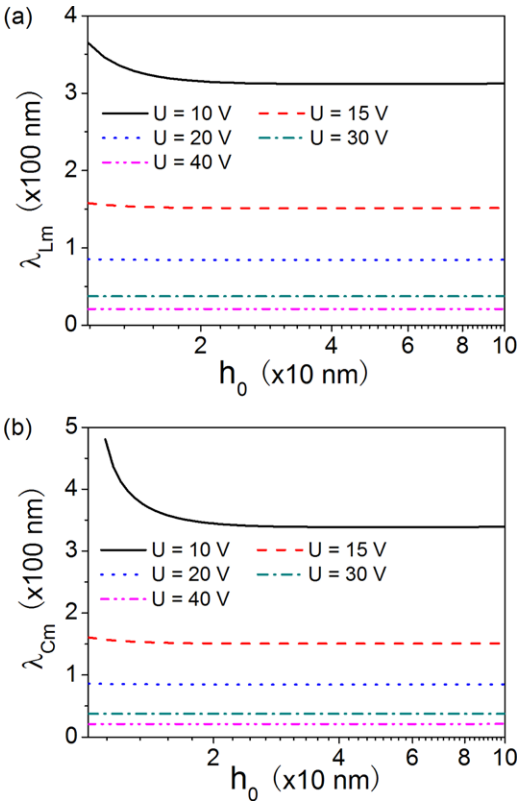


**Figure 5.** (a) Dependence of the characteristic wavelength $\lambda_{Lm}$ on the film thickness $h_0$ for different voltages. (b) Dependence of the characteristic wavelength $\lambda_{Cm}$ on the film thickness $h_0$ for different voltages.

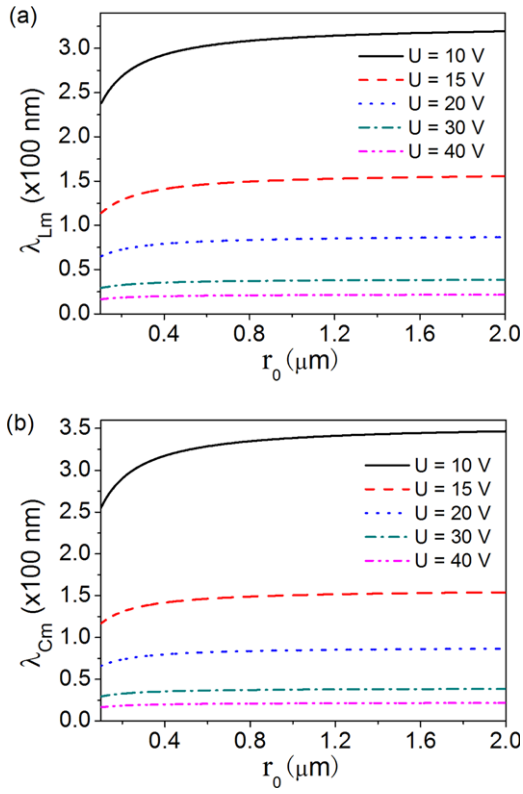


**Figure 6.** (a) Dependence of the characteristic wavelength $\lambda_{Lm}$ on the curvature radius $r_0$ for different voltages. (b) Dependence of the characteristic wavelength $\lambda_{Cm}$ on the curvature radius $r_0$ for different voltages. In the plots, $\gamma = 0.015$ N m$^{-1}$, $h_0 = 50$ nm, $d = 50$ nm [16, 31].

surface instability of the film. It is interesting to note that both $\lambda_{Lm}$ and $\lambda_{Cm}$ linearly depend on $U$ in the bi-logarithmic plot. This result is similar to that reported by Schäffer *et al* [11, 13] who found that in reduced coordinates, the wavelength of a planar film linearly decreases with the electric field intensity.

Figure 5 plots the dependences of the wavelengths $\lambda_{Lm}$ and $\lambda_{Cm}$ on the film thickness, where we use $\gamma = 0.015$ N m$^{-1}$, $d = 50$ nm, $A = -20 \times 10^{-20}$ J [16, 31] and $r_0 = 1$ $\mu$m. With the increase in the film thickness both $\lambda_{Lm}$ and $\lambda_{Cm}$ decrease gradually and then approach constants. However, the thickness effect on the characteristic pattern can be neglected when the voltage is large enough.

When the fiber size reduces to a relatively small scale (e.g. 1 $\mu$m), the surface wrinkling behavior sensitively depends on the curvature radius $r_0$, as illustrated in figure 6. One can find that under a given voltage, the smaller the fiber radius, the shorter the surface wrinkling wavelength, especially for a fiber with a diameter smaller than 1 $\mu$m and under a low voltage. This curvature dependence can also be suppressed by a strong applied electric field. When the voltage is sufficiently high (e.g. $U = 40$ V), the electric field prevails over the surface tension and van der Waals interaction and completely dominates the surface patterning behavior. Therefore, for a very high voltage, the effect of both film thickness and fiber curvature on the surface morphology can be neglected and the solution reduces to that for a thin film on a planar substrate.

We take the circumferential instability for example to observe the effect of the surface tension of the film. Figure 7

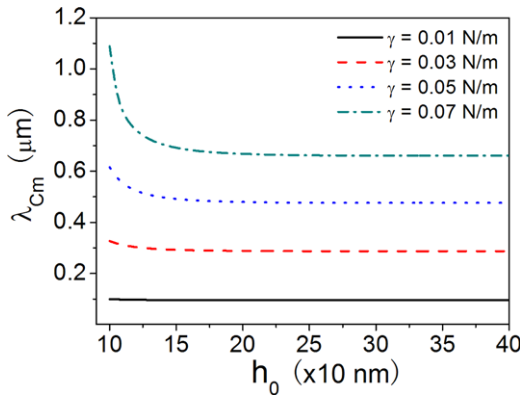


**Figure 7.** Dependence of the characteristic wavelength $\lambda_{Cm}$ on the film thickness $h_0$ for different surface tensions $\gamma$. In the plot, $U = 15$ V, $r_0 = 0.5$ $\mu$m, $d = 50$ nm.

reveals that the surface tension magnifies the wavelength of surface patterns. It is worth mentioning that the surface tension plays a stabilizing role in a planar film while it can also result in spontaneous instability in the longitudinal direction for a thin film on a microsized fiber, as already described in section 4. The surface tension can drive the Rayleigh-like instability of the cylindrical film surface with a characteristic wavelength $2\sqrt{2}\pi b$, and the electric field reduces this wavelength.

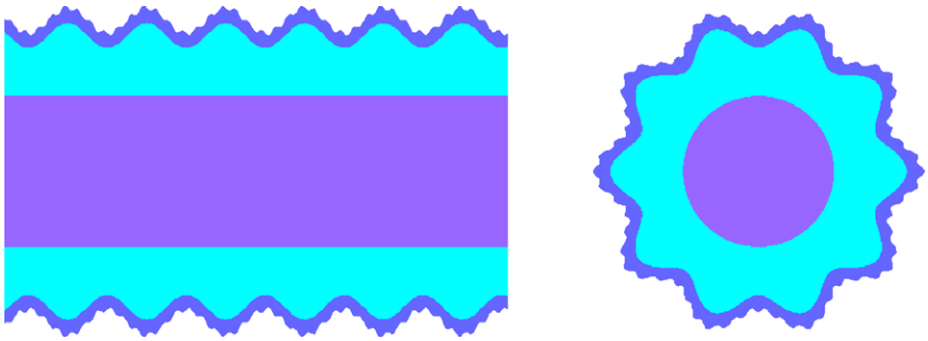

**Figure 8.** Hierarchical patterns on a cylinder.

## 5. Possible applications

The surface wettability of a material relies not only on its chemical composition but also on its surface morphology. Various interesting phenomena and superior surface properties of materials occur when the characteristic sizes of their surface structure materials reduce to micro- or nanometers, for example the superhydrophobicity of lotus leaves [1], water striders [2, 32] and mosquitoes [33]. These surface properties are not only crucial for various biological processes but are also attractive for numerous industrial applications, for instance easy-cleaning windows and traffic indicators (to repel raindrops), antisticking antennas for snow and stain-resistant textiles, aquatic super-floating and drag-reducing coatings for miniature aquatic robots and hulls. Therefore, much effort has been given to fabricating hierarchical micro/nanostructures on solid surfaces, through top-down (e.g. photolithography) and bottom-up (e.g. molecular self-assembly) approaches. For example, Shi *et al* [34] fabricated, by using the latter method, an artificial biomimetic water strider.

Our above theoretical analysis suggests that surface patterns with controllable characteristic sizes can also be fabricated on a polymer film lying on a cylinder by applying an external electric field. In addition, this method can be employed in, for example, biomimetic fabrication of a fiber with hierarchical structures like those on water strider legs. The fabrication of such a hierarchical surface structure could be achieved via a two-step approach, as depicted in figure 8. First, we introduce a viscous polymer film coating on a stiff fiber and then pattern its surface with a microsized wavelength by applying an electric field at a relatively high temperature. After the patterned polymer has been solidified, another thinner polymer melt film is coated. In the second step, the outermost thin film surface is patterned with a nanosized wavelength by applying an electric field with a designed amplitude.

## 6. Conclusions

A linear instability analysis has been presented for a viscous fluid film lying on a stiff cylinder. The equation for evolution of the film surface morphology with time and the critical condition of instability are provided analytically. It is found that the characteristic wrinkling wavelength, corresponding to the maximum growth rate of surface perturbation, decreases with increase in the externally applied voltage. The original curvature radius of the film plays a significant role in the surface instability, especially when it reduces to micro/nanosizes. The surface tension destabilizes the film surface with Rayleigh-like characteristics, which is distinct from those occurring on the planar film.

Some recent previous studies suggested that surface instability and pattern formation can occur on planar films in response to such interactions as the van der Waals or electrostatic force, which can be induced by a rigid contactor [5, 9]. However, this technique encounters difficulties when it is applied to curved surfaces. Our analysis in the present paper indicates that an applied electric field might be utilized to pattern a curved surface. By varying the intensity of the electric field, the characteristic sizes of the patterning on the surface of a curved film could be mediated. Therefore, this study is helpful for fabricating micro/nanopatterns and hierarchical patterns on the surfaces of materials and devices.

## Acknowledgments

The supports from the National Natural Science Foundation of China (grant nos 10972121, 10525210 and 10732050) and the 973 Program of MOST (grant no. 2010CB631005) are acknowledged.

## References

[1] Blossey R 2003 Self-cleaning surfaces-virtual realities *Nat. Mater.* **2** 301
[2] Feng X Q, Gao X, Wu Z, Jiang L and Zheng Q S 2007 Superior water repellency of water strider legs with hierarchical structures: experiments and analysis *Langmuir* **23** 4892
[3] Herminghaus S, Jacobs K, Mecke K, Bischof J, Fery A, Ibn-Elhaj M and Schlagowski S 1998 Spinodal dewetting in liquid crystal and liquid metal films *Science* **282** 916
[4] Erlebacher J and Aziz M J 1999 Spontaneous pattern formation on ion bombarded Si(001) *Phys. Rev. Lett.* **82** 2330
[5] Shenoy V and Sharma A 2001 Pattern formation in a thin solid film with interactions *Phys. Rev. Lett.* **86** 119
[6] Mukhrjee R, Bandyopadhyay D and Sharma A 2008 Control of morphology in pattern directed dewetting of thin polymer films *Soft Matter* **4** 2086
[7] Cerda E and Mahadevan L 2003 Geometry and physics of wrinkling *Phys. Rev. Lett.* **90** 74302

[8] Genzer J and Groenewold J 2006 Soft matter with hard skin: from skin wrinkles to templating and material characterization *Soft Matter* **2** 310
[9] Huang S Q, Li B and Feng X Q 2008 Three-dimensional analysis of spontaneous surface instability and pattern formation of thin soft films *J. Appl. Phys.* **103** 083501
[10] Huang S Q and Feng X Q 2008 Spinodal surface instability of soft elastic thin films *Acta Mech. Sin.* **24** 289
[11] Schäffer E, Thurn-Albrecht T, Russell T P and Steiner U 2000 Electrically induced structure formation and pattern transfer *Nature* **403** 874
[12] Lin Z, Kerle T, Baker S M, Hoagland D A, Schäffer E, Steiner U and Russell T P 2001 Electric field induced instabilities at liquid/liquid interfaces *J. Chem. Phys.* **114** 2377
[13] Shäffer E, Thurn-Albrecht T, Russell T P and Steiner U 2001 Electrohydrodynamic instabilities in polymer films *Europhys. Lett.* **53** 518
[14] Harkema S and Steiner U 2005 Hierarchical patter formation in thin polymer films using an electric field and vapor sorption *Adv. Funct. Mater.* **15** 2016
[15] Wu N and Russel W B 2005 Dynamics of the formation of polymeric microstructures induced by electrohydrodynamic instability *Appl. Phys. Lett.* **86** 241912
[16] Verma R, Sharma A, Kargupta K and Bhaumik J 2005 Electric field induced instability and pattern formation in thin liquid films *Langmuir* **21** 3710
[17] Bandyopadhyay D and Sharma A 2007 Electric field induced instabilities in thin confined bilayers *J. Colloid Interface Sci.* **311** 595
[18] Bae J, Glogowski E, Gupta S, Chen W, Emrick T and Russell T 2008 Effect of nanoparticles on the electrohydrodynamic instabilities of polymer/nanoparticle thin films *Macromolecules* **41** 2722
[19] Nie Z H and Kumacheva E 2008 Patterning surfaces with functional polymers *Nat. Mater.* **7** 277
[20] Fong H, Chun I and Reneker D H 1999 Beaded nanofibers formed during electrospinning *Polymer* **40** 4585
[21] Chen J L and Hwang C C 1996 Nonlinear rupture theory of a thin liquid film on a cylinder *J. Colloid Interface Sci.* **182** 564
[22] Varea C, Aragon J L and Barrio R A 1999 Turing patterns on a sphere *Phys. Rev.* E **60** 4588
[23] Matthews P C 2003 Pattern formation on a sphere *Phys. Rev.* E **67** 036206
[24] Simitev R and Busse F H 2003 Patterns of convection in rotating spherical shells *New J. Phys.* **5** 97
[25] El-Sayed M F and Syam M I 2007 Numerical study for the electrified instability of viscoelastic cylindrical dielectric fluid film surrounded by a conducting gas *Physica* A **377** 381
[26] Li B, Feng X Q, Li Y and Wang G F 2009 Morphological instability of spherical soft particles induced by surface charges *Appl. Phys. Lett.* **95** 021903
[27] Duan H L, Weissmüller J and Wang Y 2008 Instabilities of core–shell heterostructured cylinders due to diffusions and epitaxy: spheroidization and blissom of nanowires *J. Mech. Phys. Solids* **56** 1831
[28] Schmidt V, McIntyre P C and Gosele U 2008 Morphological instability of misfit-strained core–shell nanowires *Phys. Rev.* B **77** 235302
[29] Landau L D and Lifshitz E M 1960 *Electrodynamics of Continuous Media* (Oxford: Pergamon)
[30] Rayleigh L 1878 On the instability of jets *Proc. Lond. Math. Soc.* **s1–10** 4
[31] Bandyopadhyay D, Sharma A and Shankar V 2008 Instabilities and pattern miniaturization in confined and free elastic–viscous bilayers *J. Chem. Phys.* **128** 154909
[32] Liu J L, Feng X Q and Wang G F 2007 Buoyant force and sinking conditions of a hydrophobic thin rod floating on water *Phys. Rev.* E **76** 066103
[33] Wu C W, Kong X Q and Wu D 2007 Micronanostructures of the scales on a mosquito's legs and their role in weight support *Phys. Rev.* E **76** 017301
[34] Shi F, Niu J, Liu J L, Liu F, Wang Z Q, Feng X Q and Zhang X 2007 Towards understanding why a superhydrophobic coating is needed by water striders *Adv. Mater.* **19** 2257